

Ammonia Absorption on Alkaline Earth Halides as Ammonia Separation and Storage Procedure

Chun Yi Liu^{1,2} and Ken-ichi Aika^{*,1}

¹Interdisciplinary Graduate School of Science and Engineering, Tokyo Institute of Technology, 4259 Nagatsuta, Midori-ku, Yokohama 226-8502

²CREST, JST (Core Research for Evolutional Science and Technology, Japan Science and Technology Agency), 4-1-8, Honcho, Kawaguchi 332-0012

Received June 10, 2003; E-mail: kenaika@chemenv.titech.ac.jp

For the low pressure ammonia synthesis (~ 1 MPa, 573–623 K), 40–80 kPa of ammonia produced must be separated. For this purpose, the absorption behavior of five kinds of alkaline earth metal halides (MgCl_2 , CaCl_2 , CaBr_2 , SrCl_2 , and SrBr_2) and their hydrated forms were studied under 0 to 80 kPa of ammonia at 298 to 473 K. Although the equilibrium data of the ammine complex formation of these materials are known, the absorption started at higher pressure than the equilibrium data, due to the presence of enough chemical potential $\Delta\mu$ for ammonia absorption. Initial absorption (to low numbers of coordinated ammonia) was slow and depended on the sample specific surface area. The successive absorption (beyond 1 or 2 of ammonia coordination) occurs easily and reversibly. The “quasi” absorption and desorption isotherms studied here were useful for the design of ammonia separation materials. $\text{MgCl}(\text{OH})$, CaCl_2 , and CaBr_2 were found to be practical for TSA (Temperature Swing Adsorption) material working between 298 and 473 K at 40 kPa. Especially, the ammonia separation capacity of $\text{MgCl}(\text{OH})$ (26.1 mmol g^{-1}) was 5.5 times as high as that of Na exchanged Y-zeolite.

Ammonia is now being used as a reducing agent for NO_x removal at fixed NO_x emission sites such as power plants and disposal furnaces, despite the high costs due to transportation and storage. If ammonia can be produced on-site efficiently, such technology would spread. Promoted Ru catalysts newly developed can produce ammonia under mild conditions such as 623 K and 10 bar. A new de- NO_x process with ammonia on-site synthesis has thus been proposed by our group as an answer of this problem.¹ In this process, reactors with catalysts (Ru catalyst for ammonia synthesis and V_2O_5 catalyst for ammonia SCR of NO_x) are well developed. However, an ammonia separation and storage material under 40–80 kPa of ammonia is not fully developed; this is a key for practical use of the process.

Ammonia separation and storage capacity of surface treated active carbon and ion exchanged Y-zeolites studied in the previous works are not enough; the ammonia separation and storage capacity of Cu ion exchanged Y-zeolite is approximately 5 mmol g^{-1} with TSA (temperature swing adsorption) condition, ammonia separation capacity of oxidized active carbon ($\text{H}_2\text{SO}_4\text{-AC}$) is approximately 2.6 mmol g^{-1} with PSA (pressure swing adsorption) condition.^{2–4} More effective materials, which can have higher ammonia separation and storage capacity than 20 mmol g^{-1} , must be sought. For an economical process design, PSA method is preferable to TSA method.

Any kinds of inorganic halides are well known to form ammine complexes, and these ammonia absorption properties have been studied for the use of chemical heat pump.^{5–9} CaCl_2 is used as an ammonia absorbent for a refrigeration system.^{5–7,10,11} The structures of several ammine complexes have been studied.^{12–14} However, the data obtained for chemical heat

pump system cannot be used because the ammonia pressure (1 MPa) is much higher than that for the purpose of this study.^{5–7,10,11}

These inorganic halides form stoichiometric ammine complexes, and the reaction stoichiometry can be described as follows:



This is the general form of one step in the full ammine complex formation. For the example of $\text{CaCl}_2 \cdot 8\text{NH}_3$, the reaction is divided into four: $\text{CaCl}_2 + \text{NH}_3 \rightleftharpoons \text{CaCl}_2 \cdot \text{NH}_3$, $\text{CaCl}_2 \cdot \text{NH}_3 + \text{NH}_3 \rightleftharpoons \text{CaCl}_2 \cdot 2\text{NH}_3$, $\text{CaCl}_2 \cdot 2\text{NH}_3 + 2\text{NH}_3 \rightleftharpoons \text{CaCl}_2 \cdot 4\text{NH}_3$, and $\text{CaCl}_2 \cdot 4\text{NH}_3 + 4\text{NH}_3 \rightleftharpoons \text{CaCl}_2 \cdot 8\text{NH}_3$. The equilibrium pressures of ammine complex formation to inorganic halides are obtained by the dissociation pressure measurement,^{15–20} and a part of these thermodynamic data are summarized in Table 1.^{8,21,22} Here, MgCl_2 6–2 represents a change in the number of coordinated ammonia from 2 to 6 ($\text{MgCl}_2 \cdot 2\text{NH}_3(\text{s}) + 4\text{NH}_3(\text{g}) \rightleftharpoons \text{MgCl}_2 \cdot 6\text{NH}_3(\text{s})$) in Table 1. The equilibrium for these reactions show linear relationship in $1/T$ vs $\ln P$ plots, and the relation (Clausius–Clapeyron equation) can be described as below:

$$\ln P = -\Delta H/RT + \Delta S/R \quad (2)$$

Here, ΔH and ΔS represent the enthalpy and entropy changes for the reaction, and these values have been determined from ammonia dissociation pressure of ammine complexes. Also, P_{298} indicates the calculated equilibrium pressure of ammine complex formation at 298 K. For the magnesium and calcium halides in Table 1, ΔS is almost constant in the range of

Table 1. Thermodynamic Data of Ammine Complex Formation

Sample	$\Delta H/\text{J mol}^{-1}$	$\Delta S/\text{J mol}^{-1} \text{K}^{-1}$	$P_{298}/\text{kPa}^{\text{a)}$	Reference
Chloride				
MgCl ₂ 6-2	55660	230.63	1.97×10^{-1}	21
MgCl ₂ 2-1	74911	230.30	8.04×10^{-5}	21
MgCl ₂ 1-0	87048	230.88	6.45×10^{-7}	21
CaCl ₂ 8-4	41013	230.30	69.9	21
CaCl ₂ 4-2	42268	229.92	40.3	21
CaCl ₂ 2-1	63193	237.34	2.12×10^{-2}	21
CaCl ₂ 1-0	69052	234.14	1.36×10^{-3}	21
SrCl ₂ 8-1	41431	228.80	49.3	21
SrCl ₂ 1-0	15316	131.43	15.2	22
BaCl ₂ 8-0	37665	227.25	187.0	21
Bromide				
CaBr ₂ 8-6	41647	232.72	72.4	22
CaBr ₂ 6-2	45574	221.09	3.67	22
CaBr ₂ 2-1	79037	253.82	2.58×10^{-4}	22
CaBr ₂ 1-0	71318	226.22	2.10×10^{-4}	22
SrBr ₂ 8-2	54714	259.62	9.45	22
SrBr ₂ 2-1	88706	340.78	1.82×10^{-1}	22
SrBr ₂ 1-0	36259	165.01	1.85×10^{-1}	22

a) Calculated equilibrium pressure at 298 K.

210–240 kJ mol⁻¹ K⁻¹. On the other hand, ΔH is significantly changed depending on the cation, anion species, and the number of coordinated ammonia. Among the same anion (chloride) ammine complex formation, which is described as $\text{MX}_2 + n\text{NH}_3 \rightleftharpoons \text{MX}_2 \cdot n\text{NH}_3$ (M: divalent cation), ΔH is ordered as follows: $\text{MgCl}_2 > \text{CaCl}_2$. Among the same cation (calcium) ammine complex formation, ΔH is ordered like $\text{CaCl}_2 < \text{CaBr}_2$.

If the operating temperature and pressure are determined, the proper materials for the ammonia separation might be chosen from this chart. Despite these fine data, we have to examine the data for the practical use. Two reasons are: 1) Ammine complex formation is a structural change reaction and is much controlled by the rate. 2) Some bromides and iodides are decomposed by CO₂ and/or H₂O in air. Unstable halides cannot be used as ammonia separation materials for practical use. Possible effects of crystalline water might be complicated.

In this work, five kinds of alkaline earth halides (MgCl₂, CaCl₂, CaBr₂, SrCl₂, and SrBr₂) and their hydrated forms were studied for ammonia absorbent. These samples are stable for CO₂ and/or H₂O in air. The ammonia absorption and desorption behavior of these substances are studied. The pretreatment condition affects the ammonia absorption thus the possibilities as ammonia separation material for our purpose are discussed.

Experimental

Sample Preparation. Five kinds of alkaline earth metal halide were prepared as ammonia absorbent. MgCl₂·6H₂O (99.9%; Wako Chemicals), CaCl₂·2H₂O (99.9%; Wako Chemicals), CaBr₂·2H₂O (99.5%; Wako Chemicals), SrCl₂·6H₂O (99.9%; Wako Chemicals), and SrBr₂·6H₂O (99%; Aldrich) were used as starting substances. The authentic samples in powder form were compressed into pellets at 20 MPa for 10 min. The pellets were crushed and sieved to grains with diameters of about 2 mm. Before the experiment, each sample grain was evacuated for 2 h at either 723, 523, or 298 K as pretreatment. Here, pretreated sample is de-

scribed as CaCl₂(723), for example, if CaCl₂·2H₂O is evacuated at 723 K.

Sample Characterization. The dehydration behavior of alkaline earth metal halide hydrate was estimated by TG method. TG measurement (SSC/5200; Seiko Instruments) was carried out from room temperature (about 298 K) to 873 K with 10 K min⁻¹ of temperature ramping rate and 50 mL min⁻¹ of N₂ flow.

The specific surface area of CaCl₂(723) and CaCl₂(523) was measured by BET method with Kr adsorption at 77 K (BELSORP 28SA; BEL Japan).

Ammonia Absorption and Desorption Measurement. The ammonia absorption and desorption isotherms were obtained by volumetric method with an automatic gas adsorption apparatus (OMNISORP 100CX; Beckman Coulter). 50 mg of samples was placed at the sample cell and then pretreated at either 723, 523, or 298 K (3 samples) with evacuation (at $<10^{-3}$ Pa) for 2 h. The observed “quasi equilibrium” pressure was defined as the pressure at which the pressure change in 40 sec becomes smaller than 0.2 Torr (27 Pa). In this measurement condition, about 15 min are required to obtain an “quasi” equilibrium point including valve operations, and about 24 h are required to finish the whole measurement. Generally, absorption of gaseous ammonia by the salt through ammine complex formation is extremely slow, and a long absorption time such as 24 h is employed to obtain CaCl₂·8NH₃ in a true equilibrium condition.^{16,20} Accordingly, the absorption time to obtain a “quasi equilibrium” in this study is shorter than the reported works. In other words, the obtained “quasi equilibrium” pressure does not agree to the equilibrium pressure calculated from Eq. 2.

Each ammonia absorption–desorption “quasi” isotherm was measured between 0 and 80 kPa at 298 and 473 K, and the measurements were done two times for each isotherm. The amount of ammonia absorbed at the first measurement was denoted as the total absorption. The sample was evacuated to remove ammonia at the same temperature for 1 h, then the second absorption was carried out. The ammonia absorption amount of the second was denoted as the reversible absorption. Here, reversibly absorbed ammonia indicates that it can be desorbed by desorption cycle and evacua-

tion operation, and irreversibly absorbed ammonia indicates that it cannot be desorbed by desorption cycle and evacuation operation, in this experimental condition.

Results

Form of Samples after Pretreatment at Different Temperatures. The actual chemical forms of each sample were estimated by TG measurement, and are summarized in Table 2. TG profiles of each sample are shown in Fig. 1. The weight decreases of $\text{CaCl}_2 \cdot 2\text{H}_2\text{O}$, $\text{CaBr}_2 \cdot 2\text{H}_2\text{O}$, $\text{SrCl}_2 \cdot 6\text{H}_2\text{O}$, and $\text{SrBr}_2 \cdot 6\text{H}_2\text{O}$ indicate that these samples are dehydrated above 523 K. However, only $\text{MgCl}_2 \cdot 6\text{H}_2\text{O}$ did not complete the dehydration up to 723 K. Figure 2 shows the TG profiles of $\text{MgCl}_2 \cdot 6\text{H}_2\text{O}$ where the temperature rise is stopped and the temperature is kept for 2 h at 523 or 723 K. The weight up to 523 K was 41.0% of $\text{MgCl}_2 \cdot 6\text{H}_2\text{O}$, suggesting formation of $\text{MgCl}(\text{OH})$ (ideally 37.8%). Also, the weight up to 723 K was 25.5% of $\text{MgCl}_2 \cdot 6\text{H}_2\text{O}$, suggesting formation of a mixture of $\text{MgCl}(\text{OH})$ and MgO ($\text{MgCl}_{0.32}\text{OH}_{0.32}$).^{23–25}

Table 2. Form of Alkaline Earth Metal Halide Hydrate Estimated from TG Measurement

Name of sample	Actual form	Molecular weight ^{a)} / g mol^{-1}
$\text{MgCl}_2(723)$	$\text{MgCl}_{0.32}\text{OH}_{0.32}$ ^{b)}	51.84
$\text{MgCl}_2(523)$	$\text{MgCl}(\text{OH})$	76.77
$\text{MgCl}_2(298)$	$\text{MgCl}_2 \cdot 6\text{H}_2\text{O}$	203.30
$\text{CaCl}_2(723)$, $\text{CaCl}_2(523)$	CaCl_2	110.98
$\text{CaCl}_2(298)$	$\text{CaCl}_2 \cdot 2\text{H}_2\text{O}$	147.01
$\text{CaBr}_2(723)$, $\text{CaBr}_2(523)$	CaBr_2	199.89
$\text{CaBr}_2(298)$	$\text{CaBr}_2 \cdot 2\text{H}_2\text{O}$	235.92
$\text{SrCl}_2(723)$, $\text{SrCl}_2(523)$	SrCl_2	158.53
$\text{SrCl}_2(298)$	$\text{SrCl}_2 \cdot 6\text{H}_2\text{O}$	266.62
$\text{SrBr}_2(723)$, $\text{SrBr}_2(523)$	SrBr_2	247.43
$\text{SrBr}_2(298)$	$\text{SrBr}_2 \cdot 6\text{H}_2\text{O}$	355.52

a) Calculated from the results of TG. b) Mixture of $\text{MgCl}(\text{OH})$ and MgO (32:68).

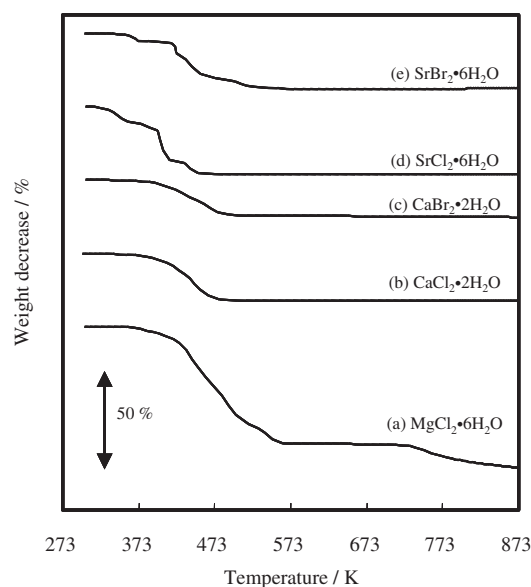


Fig. 1. TG profiles of alkaline earth metal halide hydrate.

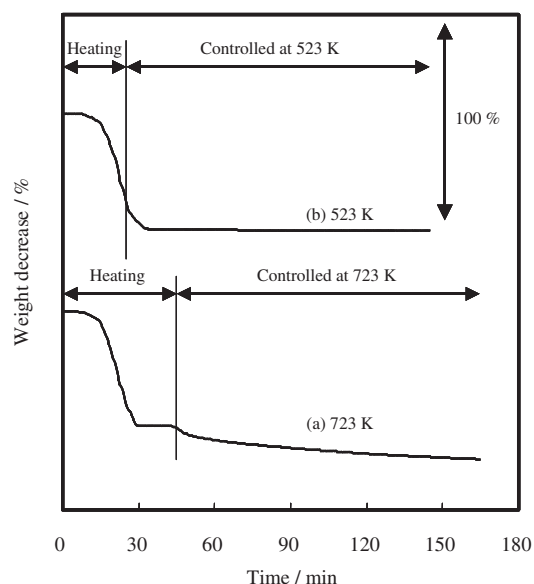


Fig. 2. TG profiles of $\text{MgCl}_2 \cdot 6\text{H}_2\text{O}$ with temperature controlling at 723 K (a) and 523 K (b).

Ammonia Absorption–Desorption Behavior of Alkaline Earth Metal Halide. Ammonia absorption (or desorption) is ammine complex formation (or decomposition). The number of coordinated ammonia with host cation was determined from the ammonia absorption and desorption isotherm. The number of coordinated ammonia N was calculated as

$$N = V \cdot M_w / 1000 \quad (3)$$

Here V and M_w mean amount of absorbed ammonia (mmol g^{-1}) and sample molecular weight (g mol^{-1}), respectively.

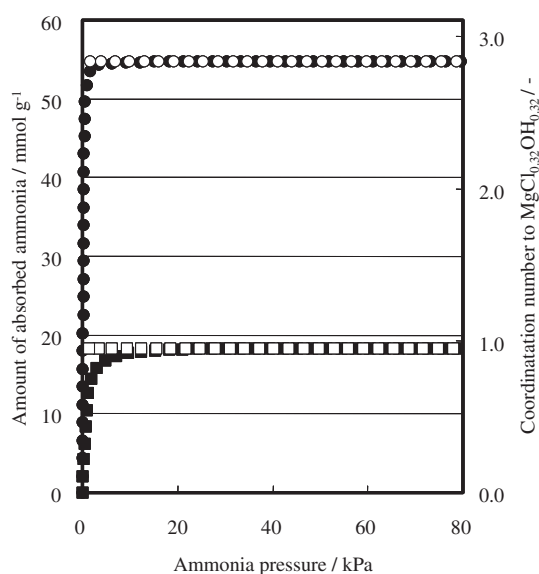
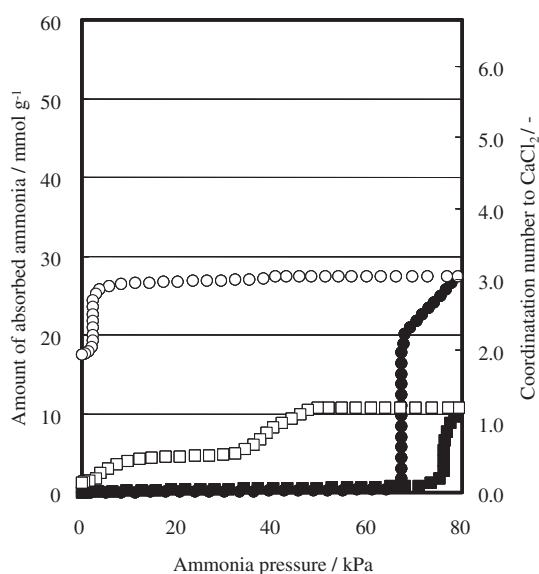
Most of the isotherms look like stepwise. Thus, it is rather easy to summarize the results (Table 3). Here, the absorbed amounts at 40, 60, and 80 kPa for absorption cycle (V_{abs}) and those at 20, 10, and 5 kPa for desorption cycle (V_{des}) at 298 K are shown. At the same time, the pressures at the step position are also shown as P_{abs} for absorption cycle and as P_{des} for desorption cycle, respectively.

The ammonia absorption “quasi” isotherms of alkali earth metal halides and the number of coordinated ammonia to these samples after 723 K pretreatment are shown in Figs. 3–9. Sample weight was defined as the sample amount after pretreatment. $\text{MgCl}_2(723)$ absorbs ammonia and is saturated with 55 mmol of ammonia for 1 g sample, with an actual form of $\text{MgCl}_{0.32}\text{OH}_{0.32}$, at a low pressure such as 5 kPa (Fig. 3). The average number of coordinated ammonia with $\text{MgCl}_2(723)$ was 2.8 for first absorption and 1.0 for second absorption.

Ammonia absorption and desorption of $\text{CaCl}_2(723)$ (actual form as CaCl_2), $\text{CaCl}_2(523)$ (actual form as CaCl_2), and $\text{CaCl}_2(298)$ (actual form as $\text{CaCl}_2 \cdot 2\text{H}_2\text{O}$) were measured at 298 K; the results are shown in Figs. 4, 5, and 6, respectively. Ammonia absorption (and desorption) isotherm has one or more steps for each sample, suggesting some structure changes. However, the pressure at which the transitions take place varied with the hydration number or structure of these pretreated samples. The pressure to evoke the first absorption is high for well-dehydrated CaCl_2 : $\text{CaCl}_2(723)$ (67 kPa) > $\text{CaCl}_2(523)$ (29

Table 3. Ammonia Absorption Capacity (V_{abs} , V_{des}) and Phase Changing Pressure (P_{abs} , P_{des}) of Alkaline Earth Metal Halides at 298 K

Sample	Run	Absorption cycle				Desorption cycle			
		P_{abs} /kPa	$V_{\text{abs}}/\text{mmol g}^{-1}$			P_{abs} /kPa	$V_{\text{des}}/\text{mmol g}^{-1}$		
			40 kPa	60 kPa	80 kPa		20 kPa	10 kPa	5 kPa
MgCl_2 (723)	1st	0.1	54.8	54.8	54.8	n.d.	54.8	54.8	54.8
	2nd	0.8	18.3	18.3	18.3	n.d.	18.3	18.3	18.3
MgCl_2 (523)	1st	1.1	36.8	38.0	38.9	n.d.	38.9	38.8	38.6
	2nd	0.3	9.1	10.0	10.8	n.d.	10.8	10.6	10.4
MgCl_2 (298)	1st	0.4, 35.9, 64.9	13.5	24.7	36.6	53.4, 27.9, 18.1, 13.3	30.3	10.6	9.4
	2nd	66.3, 67.5	0.4	1.3	24.6	38.7	1.6	1.2	1.1
CaCl_2 (723)	1st	67.3	0.2	0.4	27.5	2.4	26.8	26.6	26.0
	2nd	76.2	0.5	0.7	10.8	38.2, 3.5	4.6	4.0	2.8
CaCl_2 (523)	1st	29.3, 74.2	14.2	18.2	38.0	56.2, 5.7	30.6	29.7	21.4
	2nd	76.6	0.5	0.6	13.2	47.0, 6.4	4.8	3.7	1.7
CaCl_2 (298)	1st	11.4, 49.2, 69.0	7.1	14.7	23.2	40.9, 9.2	14.0	12.1	6.6
	2nd	45.4	0.6	14.0	22.2	50.9, 46.8	7.1	6.9	6.6
CaBr_2 (723)	1st	7.6	28.8	29.1	29.4	n.d.	29.0	28.9	28.9
	2nd	4.8	19.4	19.8	20.1	n.d.	19.6	19.5	19.4
CaBr_2 (523)	1st	0.7, 5.5	27.9	28.1	28.2	n.d.	28.2	28.2	28.2
	2nd	4.7	18.6	18.7	18.9	n.d.	18.9	18.9	18.9
CaBr_2 (298)	1st	0.5, 4.8	3.7	5.0	5.7	2.9	5.7	5.7	5.7
	2nd	5.8	6.7	8.2	9.2	3.6	9.2	9.2	9.2
SrCl_2 (723)	1st	n.d.	0.3	0.5	1.9	n.d.	0.8	0.7	0.7
	2nd	n.d.	0.2	0.4	1.0	45.3	0.4	0.4	0.4
SrCl_2 (523)	1st	68.2	0.2	0.8	6.8	33.6	4.0	3.9	3.9
	2nd	70.2, 78.7	0.2	0.3	26.3	37.4	3.5	3.5	3.4
SrCl_2 (298)	1st	39.5	2.1	4.9	5.2	34.8	1.6	1.6	1.6
	2nd	41.2	0.2	4.9	5.4	35.0	0.6	0.6	0.6
SrBr_2 (723)	1st	14.9	30.6	30.7	30.7	6.2	30.7	30.7	8.6
	2nd	10.9	22.8	22.9	23.1	5.9	23.1	23.1	1.7
SrBr_2 (523)	1st	10.2	28.8	28.9	29.1	6.5	29.4	29.4	7.9
	2nd	11.1	21.6	21.8	21.9	6.3	21.9	21.8	0.4
SrBr_2 (298)	1st	3.2, 8.0	24.4	24.4	24.4	7.3	24.4	24.4	7.0
	2nd	2.5, 8.0	23.6	23.6	23.6	7.3	23.6	23.6	5.4

Fig. 3. Ammonia absorption (closed symbol) and desorption (open symbol) isotherm of $\text{MgCl}_2(723)$ measured at 298 K; (●, ○) 1st measurement, (■, □) 2nd measurement.Fig. 4. Ammonia absorption (closed symbol) and desorption (open symbol) isotherm of $\text{CaCl}_2(723)$ measured at 298 K; (●, ○) 1st measurement, (■, □) 2nd measurement.

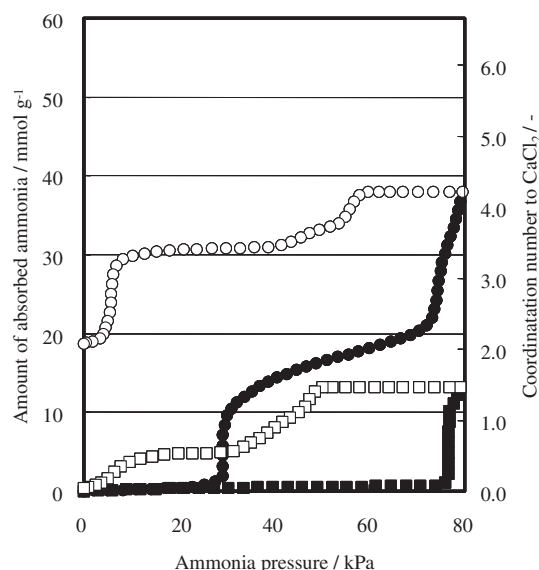


Fig. 5. Ammonia absorption (closed symbol) and desorption (open symbol) isotherm of $\text{CaCl}_2(523)$ measured at 298 K; (\bullet, \circ) 1st measurement, (\blacksquare, \square) 2nd measurement.

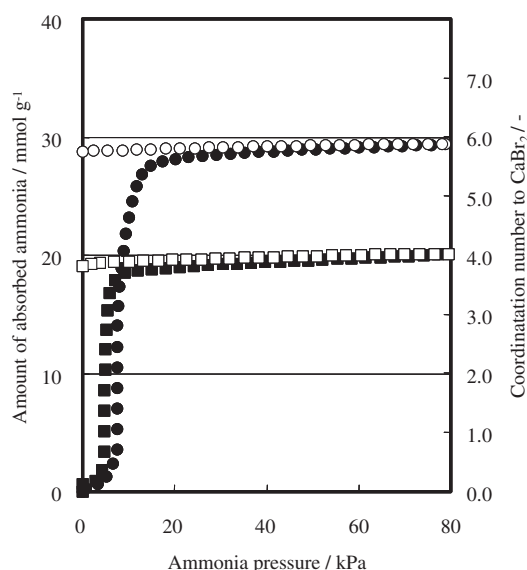


Fig. 7. Ammonia absorption (closed symbol) and desorption (open symbol) isotherm of $\text{CaBr}_2(723)$ measured at 298 K; (\bullet, \circ) 1st measurement, (\blacksquare, \square) 2nd measurement.

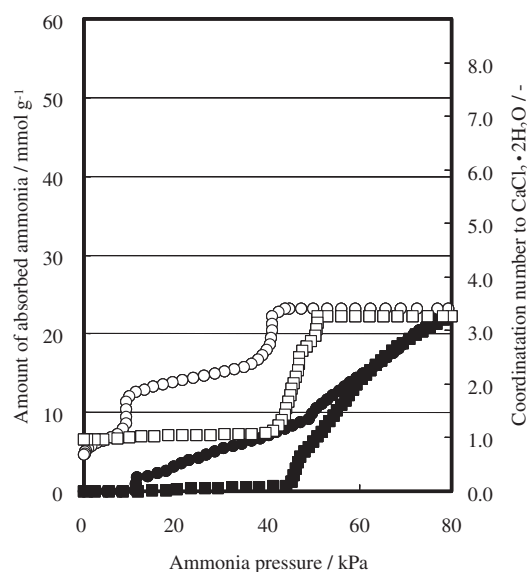


Fig. 6. Ammonia absorption (closed symbol) and desorption (open symbol) isotherm of $\text{CaCl}_2(298)$ measured at 298 K; (\bullet, \circ) 1st measurement, (\blacksquare, \square) 2nd measurement.

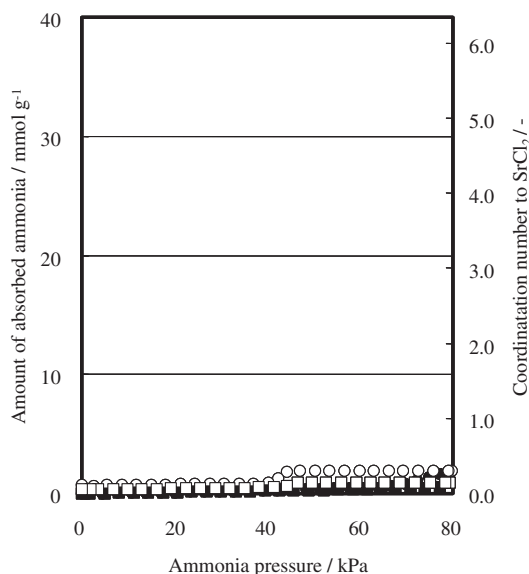


Fig. 8. Ammonia absorption (closed symbol) and desorption (open symbol) isotherm of $\text{SrCl}_2(723)$ measured at 298 K; (\bullet, \circ) 1st measurement, (\blacksquare, \square) 2nd measurement.

kPa). These pressures are surprisingly much higher than the equilibrium value calculated from Eq. 2 (1.36×10^{-3} kPa). However, the step pressures for second absorption were almost identical (74–77 kPa) for samples of $\text{CaCl}_2(723)$ and $\text{CaCl}_2(523)$.

The difference of the step pressure in first absorption indicates that the sample treated at 723 K has less affinity to ammonia or the rate process is slower than those for 523 K treated samples. From the results of Kr adsorption, the specific surface area of $\text{CaCl}_2(723)$ and $\text{CaCl}_2(523)$ were $0.776 \text{ m}^2 \text{ g}^{-1}$ and $2.77 \text{ m}^2 \text{ g}^{-1}$. It is thought that ammonia absorption is kinetically easy for the sample with higher surface area, because the absorption starts at the Ca^{2+} with unsaturated coordination at

the surface. Then, the step pressure of ammonia absorption may go down even further with the increase of surface area.

The number of coordinated ammonia with these dehydrated samples was close to 2 for first measurement and 0 for second measurement at the end of desorption (3 kPa). This indicates that 2 mol of ammonia irreversibly coordinated to 1 mol of CaCl_2 in the experimental condition of this work. If all of coordinated ammonia is removed during the first desorption cycle and evacuation, the number of coordinated ammonia at the end of the second desorption cycle must be nearly the same as at the end of the first one. These reactions was summarized as below:

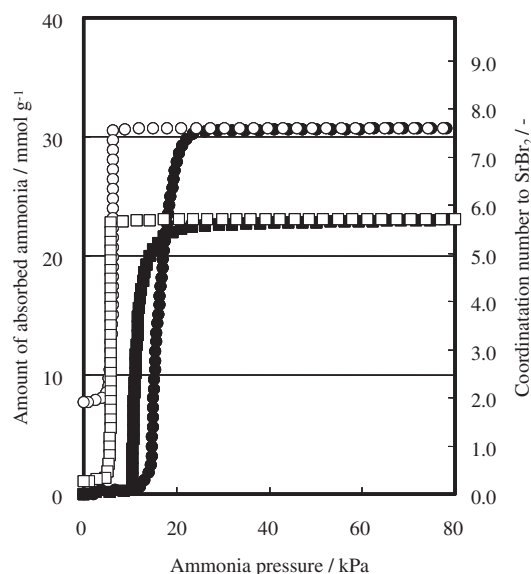
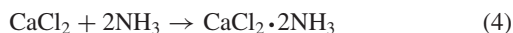


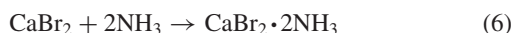
Fig. 9. Ammonia absorption (closed symbol) and desorption (open symbol) isotherm of $\text{SrBr}_2(723)$ measured at 298 K; (●,○) 1st measurement, (■,□) 2nd measurement.



In the first measurement (for fresh CaCl_2), reaction 4 (forward reaction) and 5 (reversible reaction) proceed, however, the backward reaction of 4 does not occur due to the stable ammine complex formation of $\text{CaCl}_2 \cdot 2\text{NH}_3$. In the second measurement, the starting material is $\text{CaCl}_2 \cdot 2\text{NH}_3$; only reaction 5 (reversible reaction) proceeds.

Absorption and desorption behavior of $\text{CaCl}_2(298)$, with the actual form of $\text{CaCl}_2 \cdot 2\text{H}_2\text{O}$, were quite different from completely dehydrated samples, $\text{CaCl}_2(723)$ and $\text{CaCl}_2(523)$ (Fig. 6).

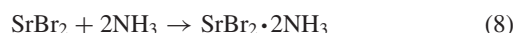
$\text{CaBr}_2(723)$, with the actual form of CaBr_2 , absorbs ammonia and reaches 23 mmol g^{-1} at 10 kPa (Fig. 7). The pressure to start the first absorption for $\text{CaBr}_2(723)$ is 7.6 kPa. However, for second absorption the step pressure is 4.7 kPa. This tendency is similar to the results of CaCl_2 . The number of coordinated ammonia with $\text{CaBr}_2(723)$ was 6 for first measurement and 4 for second measurement at 20 kPa of desorption isotherm approximately. This indicates that 2 mol of ammonia irreversibly coordinated to 1 mol of $\text{CaBr}_2(723)$, although the first desorption cycle ended at 6 of the number of coordinated ammonia. Four mol of ammonia must be desorbed during the evacuation process before the start of second run. These results are summarized as below:



Ammonia absorption was low for $\text{SrCl}_2(723)$, with the actual form of SrCl_2 , between 0 and 80 kPa (Fig. 8) despite the calculated pressure of 15.2 kPa for initial ammonia absorption (Table 1). This suggests that $\text{SrCl}_2(723)$ cannot absorb ammonia at least below 80 kPa practically.

$\text{SrBr}_2(723)$, with the actual form of SrBr_2 , absorbs ammonia

and is saturated with 22 mmol g^{-1} at 30 kPa (Fig. 9). The pressure to start the first absorption for $\text{SrBr}_2(723)$ is 15 kPa which is higher than the calculated pressure of first absorption ($1.85 \times 10^{-1} \text{ kPa}$), but rather near to the value for multi coordination of 9.45 kPa. The number of coordinated ammonia with $\text{SrBr}_2(723)$ was close to 2 at the end of first desorption cycle, but this was 0 for the second desorption cycle. This indicates that 2 mol of ammonia irreversibly coordinated to 1 mol of $\text{SrBr}_2(723)$ in the experimental condition of this work. If all of coordinated ammonia is removed during the first desorption cycle and evacuation, the number of coordinated ammonia at the end of the second desorption cycle must be nearly the same as the first one. These reactions were summarized as below:



Discussion

Behavior of Ammonia Absorption and Desorption of Alkaline Earth Metal Halides. The equilibrium pressure of ammonia absorption and desorption is determined from Eq. 2 with reaction temperature. For the alkaline earth metal halides, it is listed in Table 1.^{21,22} The order of P_{298} for the pure alkaline earth metal chlorides is BaCl_2 8–0 (187 kPa) > SrCl_2 1–0 (15.2 kPa) > CaCl_2 1–0 ($1.36 \times 10^{-3} \text{ kPa}$) > MgCl_2 1–0 ($6.45 \times 10^{-7} \text{ kPa}$). A halide of a light alkaline earth metal has higher affinity to ammonia. Also, for the pure alkaline earth metal bromide, P_{298} is higher for SrBr_2 1–0 ($1.85 \times 10^{-1} \text{ kPa}$) than for CaBr_2 1–0 ($2.10 \times 10^{-4} \text{ kPa}$). Among the same alkaline earth metals, the affinity to ammonia of bromide is higher than that of chloride.

For all dehydrated halides (CaCl_2 , CaBr_2 , SrCl_2 , and SrBr_2), the obtained pressure at the step (abrupt increase of ammonia absorption) was higher than the calculated equilibrium pressure (Table 1). This means that our measurements are apart from the “real” equilibrium condition. However, the order of the obtained pressure reflects the ammonia affinity expected from the calculated pressure. On the other hand, the obtained desorption (step) pressure was lower than the calculated pressure, suggesting that the process is not in equilibrium. Ammonia absorption (and desorption) of alkaline earth metal halides is accompanied with structure change due to the ligand addition and exchange between halogen and ammonia. For instance, the lattice constant and the structure of CaCl_2 (fresh sample) and $\text{CaCl}_2 \cdot 2\text{NH}_3$ (ammonia absorbed) are quite different;^{13,26} furthermore, the grain disintegration of fresh sample is observed during the first ammonia absorption measurement.

This indicates that the rate factors such as excess ammonia pressure and grain morphology are required to promote the absorption (and desorption). The driving force for ammonia absorption to metal salt is afforded by the difference between the chemical potential of ammonia in the gas phase, $\mu_{\text{NH}_3, \text{gas}}$, and the chemical potential of ammonia equilibrated with the solid phase, $\mu_{\text{NH}_3, \text{solid}}$. Here, $\mu_{\text{NH}_3, \text{gas}} = RT \cdot \ln P_{\text{NH}_3, \text{gas}}$ and $\mu_{\text{NH}_3, \text{solid}} = RT \cdot \ln P_{\text{NH}_3, \text{solid}}$, respectively. The fictitious pressure of ammonia equilibrated with the solid phase, $P_{\text{NH}_3, \text{solid}}$, is considered to be the equilibrium pressure of each ammonia absorption reaction calculated from Eq. 2.

Therefore, the driving force $\Delta\mu$ is expressed as follows:

$$\begin{aligned}\Delta\mu &= \mu_{\text{NH}_3, \text{gas}} - \mu_{\text{NH}_3, \text{solid}} \\ &= RT \cdot \ln(P_{\text{NH}_3, \text{gas}}/P_{\text{NH}_3, \text{solid}})\end{aligned}\quad (10)$$

Here, R and T are gas constant and temperature, respectively. In the closed system composed of ammonia and metal salt, if $\Delta\mu > 0$, ammonia absorption to metal salt will be observed; if $\Delta\mu < 0$, ammonia desorption from metal salt will be observed; and if $\Delta\mu = 0$, all components of this closed system are in "real" equilibrium condition.

Now, $\Delta\mu$ for ammonia absorption to $\text{CaCl}_2(723)$ in first measurement at 298 K is calculated below. According to Table 1, $P_{\text{NH}_3, \text{solid}}$ (P_{298} for CaCl_2 1-0) is 1.36×10^{-3} kPa, and according to Fig. 4 and Table 3, the ammonia absorption amount to $\text{CaCl}_2(723)$ is sharply increased at 67.3 kPa through the point of $N = 0.5$ (average of 0 and 1). Thus $\Delta\mu$, the driving force for initial ammonia absorption to $\text{CaCl}_2(723)$, is calculated as 26.8 kJ mol^{-1} in this experimental condition.

In the same manner, $\Delta\mu$ for $\text{CaCl}_2 \cdot \text{NH}_3 + \text{NH}_3 \rightarrow \text{CaCl}_2 \cdot 2\text{NH}_3$ (shown as CaCl_2 2-1) and $\text{CaCl}_2 \cdot 2\text{NH}_3 + 2\text{NH}_3 \rightarrow \text{CaCl}_2 \cdot 4\text{NH}_3$ (shown as CaCl_2 4-2) are also calculated as 20.0 kJ mol^{-1} and 1.7 kJ mol^{-1} , respectively. One interesting finding is that these values are not near each other. This suggests that the rate process may depend on the structure change a lot. The values of $\Delta\mu$ for each sample in the first measurement at 298 K are summarized in Table 4. High $\Delta\mu$ for a process means that the reaction is hard, probably causing a lot of disturbance to the structure of Ca^{2+} region.

Model of Ammonia Absorption to Metal Halide with Ammine Complex Formation. A model of the difference of ammonia absorption behavior between CaCl_2 and $\text{CaCl}_2 \cdot 2\text{H}_2\text{O}$ is proposed as shown in Fig. 10. The structures of these samples are quite different: slightly distorted rutile structure for CaCl_2 (a)²⁶ and layer structure for $\text{CaCl}_2 \cdot 2\text{H}_2\text{O}$ (d).²⁷ For the fresh CaCl_2 , 6 atoms of Cl^- coordinate to Ca^{2+} (a). By the complex

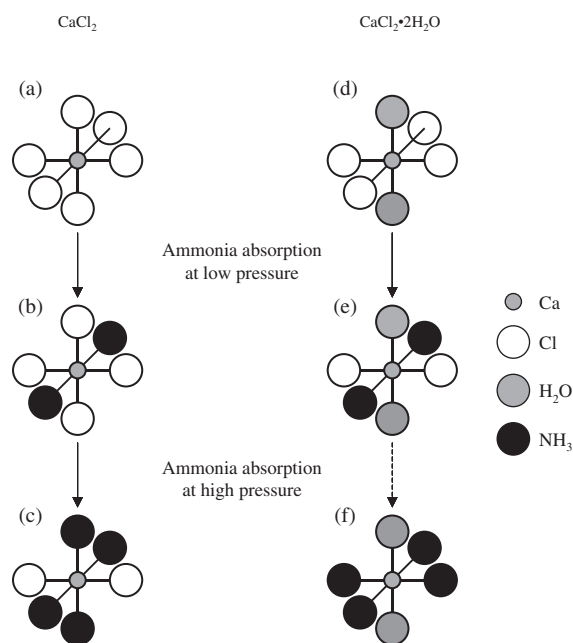


Fig. 10. The model of ammine complex formation of CaCl_2 and $\text{CaCl}_2 \cdot 2\text{H}_2\text{O}$.

formation to $\text{CaCl}_2 \cdot 2\text{NH}_3$, the number of coordinated Cl^- is changed from 6 to 4, and 2 molecules of ammonia coordinate to Ca^{2+} (b).¹³ For the complex formation to $\text{CaCl}_2 \cdot 4\text{NH}_3$, 4 molecules of ammonia and 2 atoms of Cl^- probably coordinate to Ca^{2+} (c); however, the crystal structure of $\text{CaCl}_2 \cdot 4\text{NH}_3$ had not been determined. In the case of a coordinated ammonia number between 2 and 4 (Figs. 4 and 5), the sample form may be a mixture of $\text{CaCl}_2 \cdot 2\text{NH}_3$ and $\text{CaCl}_2 \cdot 4\text{NH}_3$.

On the other hand, for the fresh $\text{CaCl}_2 \cdot 2\text{H}_2\text{O}$, 4 atoms of Cl^- and 2 molecules of water coordinate to Ca^{2+} (d). For the complex formation to $\text{CaCl}_2 \cdot 2\text{H}_2\text{O} \cdot n\text{NH}_3$, it is thought that Cl^- ions as ligand are exchanged by ammonia (e, f) with structure change. However, the details of this ammine complex formation are not clear. Here, the larger difference of initial ammonia absorption mechanism between CaCl_2 (from (a) to (b)) and $\text{CaCl}_2 \cdot 2\text{H}_2\text{O}$ (from (d) to (e)) is considered to be due to the difference of structure or to the different coordination condition of Ca^{2+} .

Rearrangement of Ammine Complex Structure with Ammonia Absorption. For CaCl_2 , CaBr_2 , and SrBr_2 , the behavior of ammonia absorption and desorption in the first cycle were different in the two samples treated after 723 and 523 K, as listed in Table 3. However, the behaviors of the second cycle were very similar for the two for each sample.

We suppose that the arrangement of ions (cation and halogen) and ammonia is changing gradually through ammonia absorption and desorption, as is shown in Fig. 10. Here, the nano size structure changes shall be discussed in view of the dehydrated sample pretreated at different temperatures.

The model of nano size structure of ammine complex during ammonia absorption and desorption is proposed as shown in Fig. 11. The grain size of the sample treated at lower temperature (a) is smaller than that treated at higher temperature (d). Ammonia absorption to the former (a, d) starts at lower pressure forming ammine complexes (b, e), and extra ammonia is

Table 4. Chemical Potential $\Delta\mu$ for Ammonia Absorption of Alkaline Earth Metal Halides at 298 K

Sample	Reaction	$\Delta\mu/\text{kJ mol}^{-1}$
$\text{CaCl}_2(723)$	CaCl_2 1-0	26.8
	CaCl_2 2-1	20.0
	CaCl_2 4-2	1.7
$\text{CaCl}_2(523)$	CaCl_2 1-0	24.7
	CaCl_2 2-1	18.5
	CaCl_2 4-2	1.5
$\text{CaBr}_2(723)$	CaBr_2 1-0	25.7
	CaBr_2 2-1	25.5
	CaBr_2 6-2	2.1
$\text{CaBr}_2(523)$	CaBr_2 1-0	20.1
	CaBr_2 2-1	21.5
	CaBr_2 6-2	1.3
$\text{SrCl}_2(523)$	SrCl_2 1-0	3.9
$\text{SrBr}_2(723)$	SrBr_2 1-0	10.7
	SrBr_2 2-1	10.9
	SrBr_2 8-2	1.5
$\text{SrBr}_2(523)$	SrBr_2 1-0	8.6
	SrBr_2 2-1	10.0
	SrBr_2 8-2	0.4

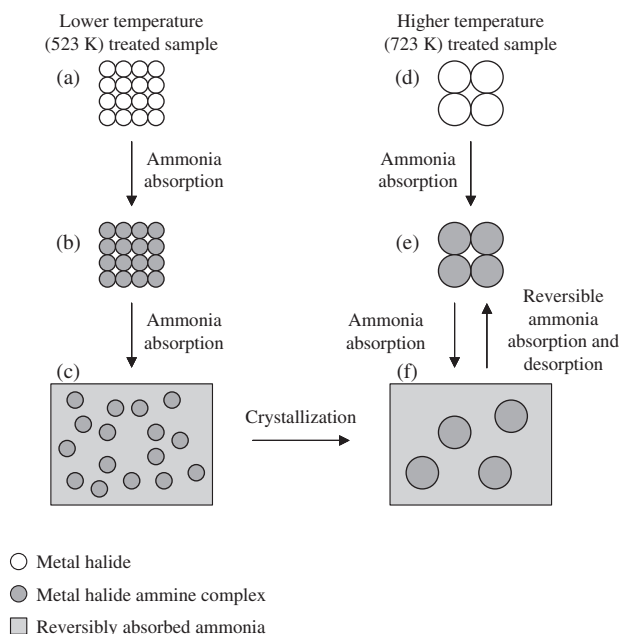


Fig. 11. The model of reconfiguration of ammine complex during ammonia absorption and desorption.

further absorbed around the grains at higher pressure (c, f). Here, the grain size affects the threshold pressure of ammonia absorption: the smaller grain accepts ammonia more easily. This explanation can be applicable to the first threshold (b, e) and the second threshold (c, f), too, as can be seen in Figs. 4 and 5.

Now, the behavior of the second cycle (reversible absorption and desorption) is very similar for the two as is seen in Figs. 4 and 5. This suggests that the crystal growth of ammine complex with smaller grain size occurs (from (c) to (f)). Even if the core complex is crystallized with large grain, some of ammonia is reversibly absorbed (coordinated at outer sphere).

If crystal growth of small-sized particles is inhibited in some way, the pressure of ammine complex formation must be close to the calculated equilibrium value.

Application of Alkaline Earth Metal Halides for TSA and PSA in Ammonia Separation. The ammonia separation capacity with respect to TSA method for alkaline earth metal halide hydrates ($\text{MgCl}_2 \cdot 6\text{H}_2\text{O}$, $\text{CaCl}_2 \cdot 2\text{H}_2\text{O}$, $\text{CaBr}_2 \cdot 2\text{H}_2\text{O}$, and $\text{SrCl}_2 \cdot 6\text{H}_2\text{O}$) treated at 523 K are shown together with those for Na form Y-zeolite (Na-Y) treated at 723 K as a reference in Fig. 12. The ammonia separation capacity with TSA was defined as the difference of total absorption amount between 298 K (absorption condition, summarized in Table 3) and 473 K (desorption condition, data are not shown) at 40 kPa. Ammonia desorption temperature of 473 K was selected from the viewpoint of waste heat utilization of ammonia synthesis (at 623 K).

The ammonia separation capacity of $\text{MgCl}_2(523)$ (with the actual form of $\text{MgCl}(\text{OH})$), $\text{CaCl}_2(523)$ (with the actual form of CaCl_2), and $\text{CaBr}_2(523)$ (with the actual form of CaBr_2) are much higher than that of Na-Y. These samples were found to be important candidates as ammonia separation material for this process with the TSA condition. Especially, the ammonia separation capacity of $\text{MgCl}_2(523)$ and $\text{CaBr}_2(523)$ were 5 times (or more) as high as that of Na-Y. On the other hand, am-

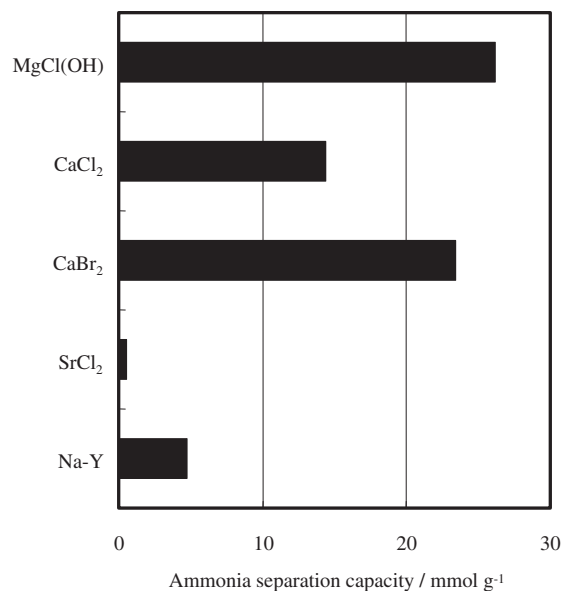


Fig. 12. Ammonia separation capacity of alkaline earth metal halides for temperature swing absorption method between 298 and 473 K, measured at 40 kPa.

monia is not absorbed to $\text{SrCl}_2(523)$, with the actual form of SrCl_2 , unless the higher pressure than 80 kPa is applied, proving that the halide of $\text{SrCl}_2(523)$ is not applicable to ammonia separation material under this condition.

Ammonia separation capacity in the working state of PSA is here defined as the difference between the amount of reversible absorption at 60–80 kPa and that at 5–10 kPa at 298 K. The ammonia separation capacity of alkaline earth metal halides with PSA method is listed in Table 5.

The 60 kPa of ammonia pressure at absorption, and 10 kPa at desorption must be practical for this purpose. For most alkaline earth metal halides, however, the amount at absorption cycle at 60 kPa was equal to or not higher than the amount at desorption cycle at 10 kPa. This indicates that these samples are not proper for ammonia separation material through PSA between 60 and 10 kPa, except for $\text{CaCl}_2(298)$ (actual form as $\text{CaCl}_2 \cdot 6\text{H}_2\text{O}$; 7.1 mmol g^{-1}) and $\text{SrCl}_2(298)$ (actual form as $\text{SrCl}_2 \cdot 6\text{H}_2\text{O}$; 4.3 mmol g^{-1}). The applicable condition of PSA is found for some alkaline earth metal halides and is shown in Table 5. $\text{SrBr}_2 \cdot 6\text{H}_2\text{O}$, as precursor of SrBr_2 type sample, with various pretreatment temperature can desorb ammonia reversibly at 6–7 kPa. Thus, these samples are applicable only when the evacuation pressure is lower than 6–7 kPa (such as 5 kPa).

The sample stability against multiple operation of absorption–desorption cycle and heating–cooling cycle was not tested in this work; thus further study of sample stability is required for practical use.

Conclusions

In this work, the ammonia absorption and desorption behavior of five kinds of alkaline earth metal halide (MgCl_2 , CaCl_2 , CaBr_2 , SrCl_2 , and SrBr_2) and their hydrated forms as alternative ammonia separation materials to surface treated active carbon and ion exchanged Y-zeolites were studied under 0 to 80 kPa at 298 to 473 K.

Table 5. Ammonia Separation Capacity of Alkaline Earth Metal Halide Hydrate for Pressure Swing Absorption Operated between 60 or 80 kPa of Absorption Pressure and 10 kPa of Desorption Pressure at 298 K

Sample	$\Delta V^a)/\text{mmol g}^{-1}$	
	Abs. at 80 kPa	Abs. at 60 kPa
MgCl ₂ (723)	0.0	0.0
MgCl ₂ (523)	0.2	0.0
MgCl ₂ (298)	23.4	0.1
CaCl ₂ (723)	6.8	0.0
CaCl ₂ (523)	9.5	0.0
CaCl ₂ (298)	15.3	7.1
CaBr ₂ (723)	0.6	0.3
CaBr ₂ (523)	0.0	0.0
CaBr ₂ (298)	0.0	0.0
SrCl ₂ (723)	0.6	0.0
SrCl ₂ (523)	22.8	0.0
SrCl ₂ (298)	4.8	4.3
SrBr ₂ (723)	0.0	0.0
SrBr ₂ (523)	0.1	0.0
SrBr ₂ (298)	0.0	0.0
SrBr ₂ (723) ^{b)}	21.4	20.5
SrBr ₂ (523) ^{b)}	21.5	21.4
SrBr ₂ (298) ^{b)}	28.2	28.2
Na-Y ^{c)}		1.3

a) Amount of absorption at 80 or 60 kPa subtracted by that at 10 kPa in the desorption cycle (from Tabel 3). b) Desorption at 5 kPa. c) As reference sample.

From the TG measurement, each alkaline earth metal halide hydrate was dehydrated by evacuation with heating. CaCl₂·2H₂O, CaBr₂·2H₂O, SrCl₂·6H₂O, and SrBr₂·6H₂O were completely dehydrated to pure halide form by evacuation up to 523 K. However, MgCl₂·6H₂O was dehydrated to MgCl(OH) at 523 K.

Ammonia absorption to each alkaline earth metal halide was eventually ammine complex formation with structure change. Under the condition of this work, some ammonia absorption was reversible. The behavior of ammonia absorption was different between alkaline earth metal species and these hydration states. The stepwise pressure of ammonia absorption for fresh alkaline earth metal halides was moved from calculated equilibrium pressure to higher pressure due to high driving force (high chemical potential $\Delta\mu$) for this process. The ammonia reversible absorption behavior of dehydrated samples was almost the same for different pretreatment temperature samples, because the rearrangement of cation (alkaline earth metal ion), anion (halogen), and ligand (ammonia) occurred during the ammonia absorption and desorption.

MgCl(OH), CaCl₂, and CaBr₂ were applicable to the ammonia separation material with TSA method between 298 and 473 K at 40 kPa. Especially, the ammonia separation capacity of MgCl(OH) (26.1 mmol g⁻¹) was 5.5 times as high as Na form Y-zeolite (4.7 mmol g⁻¹), the previously proposed ammonia separation material. However, most of these samples were not applicable to PSA method between 60 and 10 kPa at 298 K, because these samples were not able to absorb and desorb ammonia reversibly in this condition. Only CaCl₂·2H₂O (7.1

mmol g⁻¹) and SrCl₂·6H₂O (4.3 mmol g⁻¹) were applicable to PSA method at this condition; however, this ammonia separation capacity was not enough for the purpose.

During this work, the applicable ammonia separation materials with TSA were found, and it became possible to save the ammonia separation material in new de-NO_x process with ammonia on-site synthesis. Use of these samples can decrease the weight in the plant to 18% of that of Na form Y-zeolite.

This work was partially supported by Grants-in-Aid for Scientific Research (#12793002) from the Ministry of Education, Culture, Sports, Science and Technology.

References

- 1 K. Aika and T. Kakegawa, *Catal. Today*, **10**, 73 (1991).
- 2 C. Y. Liu and K. Aika, *Res. Chem. Intermed.*, **28**, 409 (2002).
- 3 C. Y. Liu and K. Aika, *Bull. Chem. Soc. Jpn.*, **74**, 1463 (2003).
- 4 C. Y. Liu and K. Aika, *J. Jpn. Pet. Inst.*, **46**, 301 (2003).
- 5 W. Wongsuwan, S. Kumar, P. Neveu, and F. Meunier, *Appl. Therm. Eng.*, **21**, 1489 (2001).
- 6 N. C. Srivastava and I. W. Eames, *Appl. Therm. Eng.*, **18**, 707 (1998).
- 7 J. Bougard, R. Jadot, and V. Poulain, "Proceedings of the International Absorption Heat Pump Conference," New Orleans, January 1993 (1994), p. 413.
- 8 I. Fujiwara, *Refrigeration*, **71**, 452 (1996).
- 9 E. Kunugita, *J. Chem. Eng. Jpn.*, **48**, 857 (1984).
- 10 S. O. Enibe and O. C. Iloje, *Renewable Energy*, **20**, 305 (2000).
- 11 B. Diawara, L. C. Dufour, and R. Hartoulari, *React. Solid*, **2**, 73 (1986).
- 12 A. Leineweber, M. W. Friedriszik, and H. Jacobs, *J. Solid State Chem.*, **147**, 229 (1999).
- 13 S. Westman, P. E. Werner, T. Schler, and W. Raldow, *Acta Chem. Scand., Ser. A*, **35**, 467 (1981).
- 14 I. Olovsson, *Acta Crystallogr.*, **18**, 889 (1965).
- 15 W. Biltz and G. F. Hüttig, *Z. Anorg. Allg. Chem.*, **119**, 115 (1921).
- 16 G. F. Hüttig, *Z. Anorg. Allg. Chem.*, **123**, 31 (1922).
- 17 G. F. Hüttig, *Z. Anorg. Allg. Chem.*, **124**, 322 (1922).
- 18 W. Stollenwerk and W. Biltz, *Z. Anorg. Allg. Chem.*, **119**, 97 (1921).
- 19 F. Ephraim, *Z. Phys. Chem.*, **81**, 513 (1913).
- 20 A. B. Hart and J. R. Partington, *J. Chem. Soc.*, **1943**, 104.
- 21 P. Neveu and J. Castaing, *Heat Recovery Syst. CHP*, **13**, 233 (1993).
- 22 "International Critical Tables of Numerical Data, Physics, Chemistry and Technology," McGraw-Hill, New York (1929), Vol. 7, pp. 224–313.
- 23 Y. Kirsh, S. Yariv, and S. Shoval, *J. Therm. Anal.*, **32**, 393 (1987).
- 24 T. Homma, *Nippon Kagaku Kaishi*, **1975**, 1512.
- 25 V. V. Sergeev and I. S. Kachanovskaya, *J. Appl. Chem. USSR*, **32**, 1708 (1959).
- 26 W. R. Busing, *Trans. Am. Crystallogr. Assoc.*, **6**, 57 (1970).
- 27 A. Leclaire and M. M. Borel, *Acta Crystallogr., Sect. B*, **33**, 1608 (1977).